

Supporting Information:

A Template-free Solvent-mediated Synthesis of High Surface Area Boron Nitride Nanosheets for Aerobic Oxidative Desulfurization

Peiwen Wu,^{a, ‡} Wenshuai Zhu,^{*, b, c, ‡} Yanhong Chao,^{b, c} Jinshui Zhang,^c Pengfei Zhang,^c Huiyuan Zhu,^c Changfeng Li,^a Zhigang Chen,^b Huaming Li,^{*, d} and Sheng Dai^{*, c}

a. School of Energy and Power Engineering, Jiangsu University, Zhenjiang 212013 (China)

b. School of Chemistry and Chemical Engineering, Jiangsu University, Zhenjiang 212013 (China)

c. Chemical Sciences Division, Oak Ridge National Laboratory, Oak Ridge, TN 37831 (USA)

d. Institute for Energy Research, Jiangsu University, Zhenjiang 212013 (China)

Experimental:

Materials: Boric acid (H_3BO_3 , AR grade), urea ($\text{CO}(\text{NH}_2)_2$, AR grade), Methanol (CH_3OH , AR grade), Ethanol ($\text{C}_2\text{H}_5\text{OH}$, AR grade), Propanol ($n\text{-C}_3\text{H}_7\text{OH}$, AR grade), Butanol ($n\text{-C}_4\text{H}_9\text{OH}$, AR grade) and decalin (AR grade) were purchased from Shanghai Sinopharm Chemical Reagent Co., Ltd. and used without purification. Dibenzothiophene (DBT, 98%) and tetradecane (99%) were purchased from Sigma-Aldrich without purification.

Characterization: Fourier Transform Infrared Spectroscopy (FT-IR) were obtained on a Nicolet Nexus 470 Fourier transform infrared spectrometer, using KBr pellets at room temperature. Ultraviolet-visible diffuse reflectance spectra (UV-DRS) were recorded on a Shimadzu UV-2450 spectrophotometer equipped with spherical diffuse reflectance accessory in the range of 200-800 nm, using BaSO_4 as the reflectance standard material. The surface morphologies of samples were analyzed by a JSM-7001F field emission scanning electron microscope (SEM), which was performed at 2-15 keV accelerating voltage. Raman tests were carried out using Thermo Scientific DXR Smart Raman spectrometer equipped with a 532 nm excitation. High resolution transmission electron microscope (HRTEM) were performed by a Hitachi H-700 Transmission Electron Microscope. Scanning transmission electron microscopy (STEM) image was performed on Nion Ultra STEM 100 (operated at 100kV). X-ray diffraction (XRD) was carried out on XRD-6100Lab (Shimadzu, Japan) equipped with Cu-K α radiation (λ) 1.5406 (Å), employing a scanning rate of $7^\circ\cdot\text{min}^{-1}$ in the 2θ range from 10 to 80° . N_2 adsorption-desorption isotherm was employed on ASAP 2460 Surface Area and Porosity Analyzer (Micromeritics, USA) to calculate the specific surface area. Atomic force microscopy (AFM, Asylum Research Company, Asylum MFP-3D) was applied to investigate the layers of materials. Meanwhile, GC-MS (Agilent 7890A-5975C) was taken to research the mechanism of adsorption coupled with oxidation of sulfur compounds.

Synthesis of nanoporous h-BNNs: A certain molar ratio of boric acid and urea (0.01 mol of H_3BO_3 mixed with 0.15 mol of urea for M-BN₁₅ and 0.30 mol of urea for other h-BNNs) in an alcohol (methanol, ethanol, propanol, butanol) was mixed with water (a mixed solution contains 20mL of alcohols and 20 mL of water). Then, the homogeneous solution was heated under 45°C for

recrystallization. A white crystalline powder product subsequently formed with the evaporation of solvents. Then, the obtained white powder was moved in a quartz boat and transformed to a tube furnace. Then the precursors were heated with a ramping rate of $5^{\circ}\text{C}\cdot\text{min}^{-1}$ to 900°C and kept for 120 min under protection of N_2 . After that, the tube furnace was naturally cooled to room temperature.

Oxidation of DBT: In a typical sulfur oxidation process, after 100 mg of h-BNNs was added to a 100 mL round-bottom flask, 40 mL of model oil (containing DBT with 500 ppm) were poured into the flask, and then the mixed solution was stirred vigorously in a thermostatic oil-bath of 150°C with air bubbled into the flask (ordinary pressure). After the reaction, the upper liquid phase samples was periodically withdrawn and separated by centrifugation before sulfur content being analyzed. The oil sample was analyzed on an gas chromatography flame ionization detection (GC-FID) (Agilent 7890A, HP-5 column, 30 m long \times 0.32 mm inner diameter (id) 0.25 μm film thickness) using tetradecane as an internal standard.

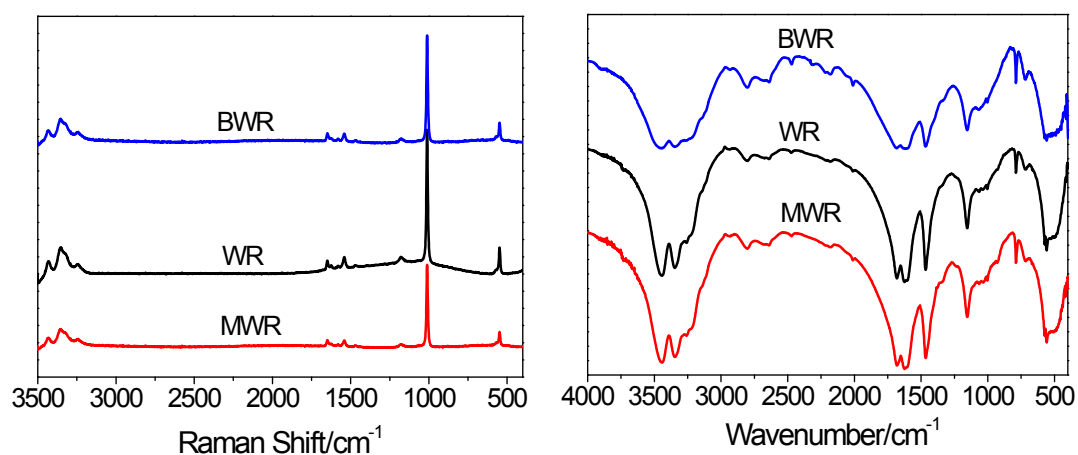


Fig. S1 Raman and FT-IR spectra of MWR, WR and BWR raw materials.

MWR, WR and BWR: three raw materials (boric acid and urea with molar ratio of 1:30, dissolve in menthol/water(MW), pure water(W) and butanol/water(BW), and sequently evaporate solvents for recrystal, producing white solid, denoted as MWR, WR and BWR, respectively).

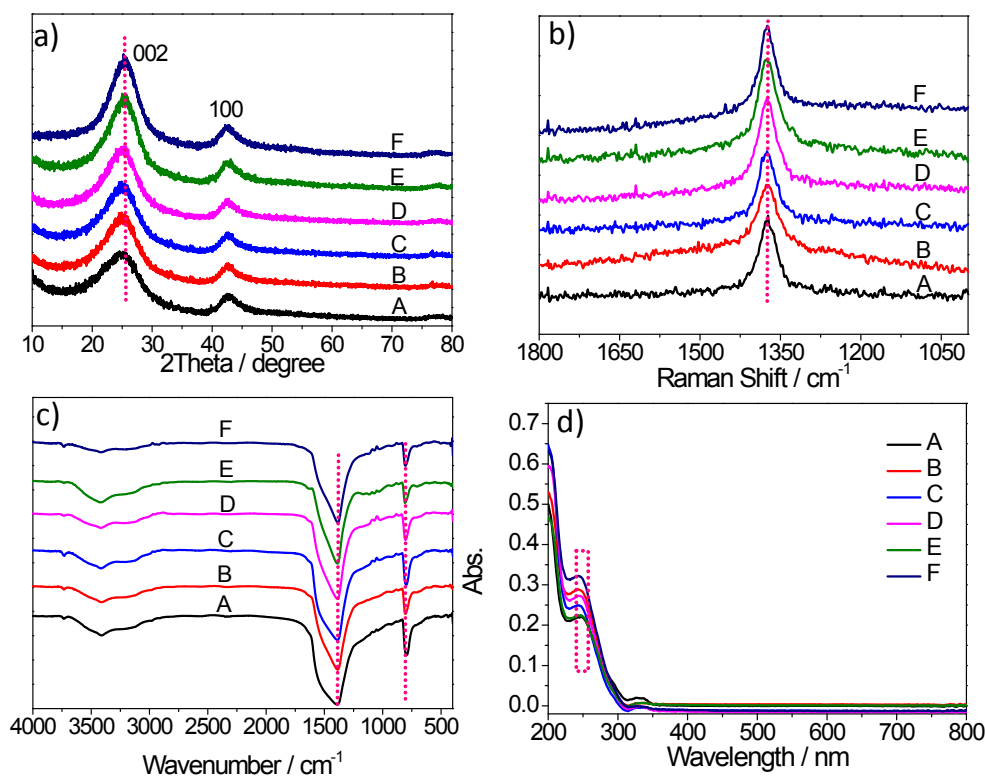


Fig. S2 Spectral characterizations of h-BNNs show no distinct changes. a) XRD patterns of h-BNNs; b) Raman spectra of h-BNNs; c) FT-IR spectra of h-BNNs; d) UV-Vis DRS spectra of h-BNNs.

Sample order: A) BN-M₃₀; B) BN-M₁₅; C) BN-E₃₀; D) BN-P₃₀; E) BN-W₃₀; F) BN-B₃₀

In XRD patterns, the results demonstrated that all the peaks of all samples are readily indexed to the standard hexagonal phase of h-BNNs (JCPDS Card 247 No. 34-0421). With melting point of solvents decrease, the peak of (002) show a slight shift to low angle, indicating the layer-layer distance is extended. The peaks at 1374 cm⁻¹ in Raman spectra are assigned to B-N vibrational mode (E_{2g}) within h-BNNs. Compared with bulk h-BN, the shift of E_{2g} peak indicates the reduction of layers. In FT-IR spectra, the peaks show no obvious difference. The peaks around 1382 cm⁻¹ and 800 cm⁻¹ are attributed to in-plane B-N transverse optical modes of hexagonal boron nitride and N-B stretching vibration modes, respectively. Moreover, UV-Vis DRS of all samples show no evident change.

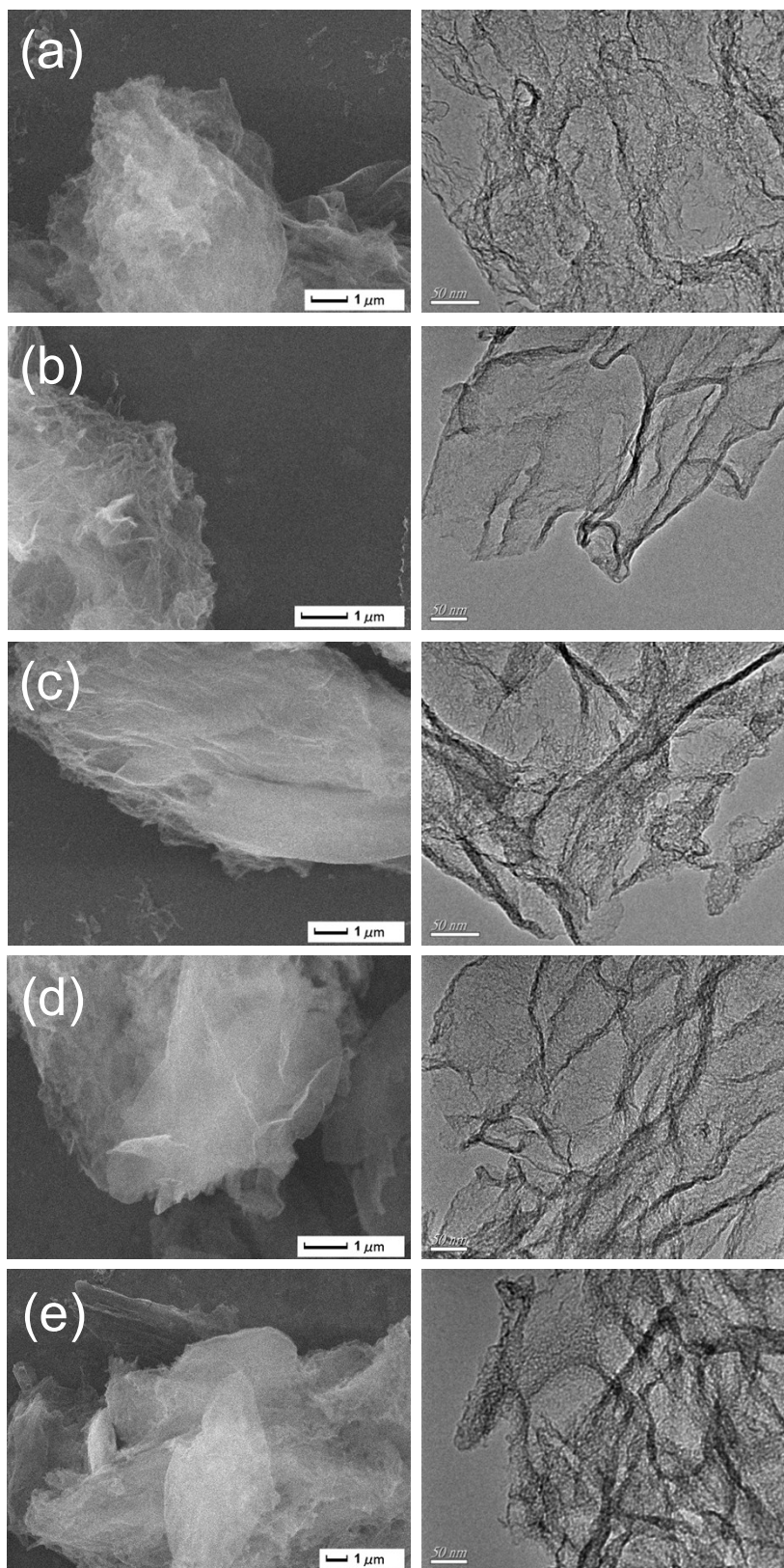


Fig. S3 SEM (left) and HRTEM (right) images of h-BNNs a) BN-M₁₅; b) BN-E₃₀; c) BN-P₃₀; d) BN-W₃₀; e) BN-B₃₀.

SEM and TEM images show that all prepared h-BNNs are thin film structure.

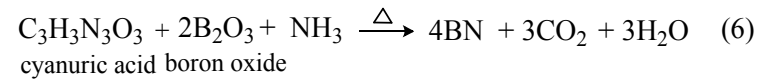
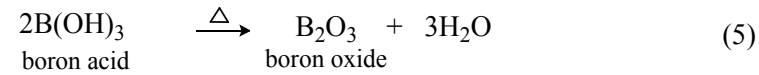
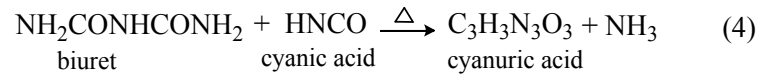
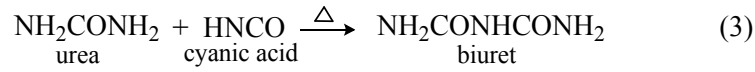
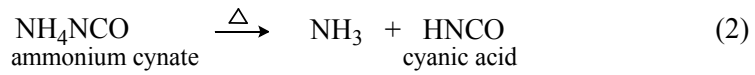


Fig. S4 The pyrolysis reaction procedure in formation of h-BNNs

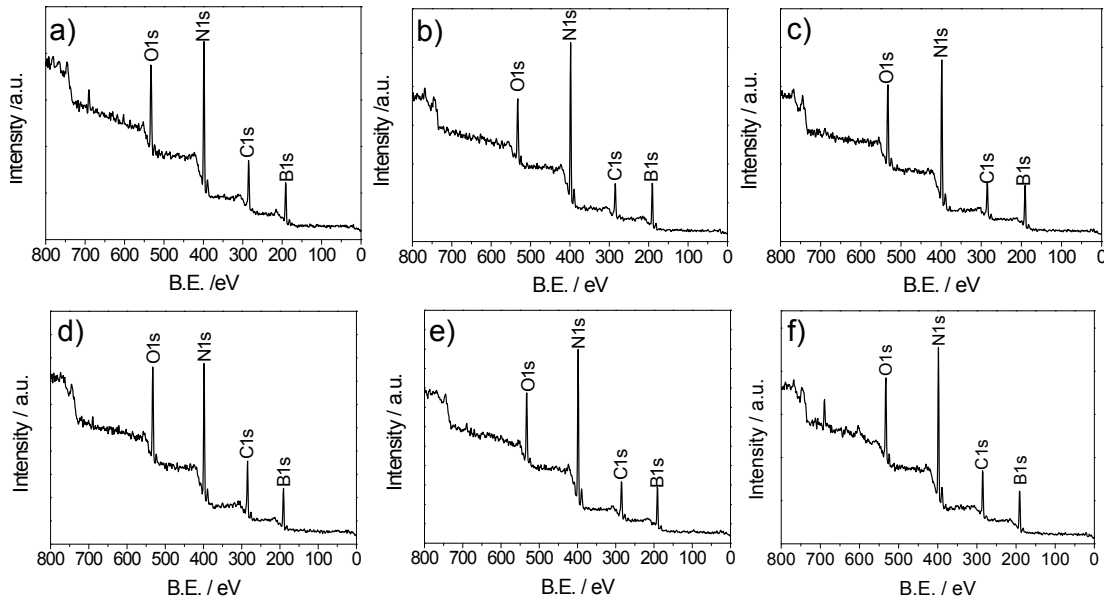


Fig. S5 XPS spectra of h-BNNs

Sample order: a) BN-M₃₀; b) BN-M₁₅; c) BN-E₃₀; d) BN-P₃₀; e) BN-W₃₀; f) BN-B₃₀.

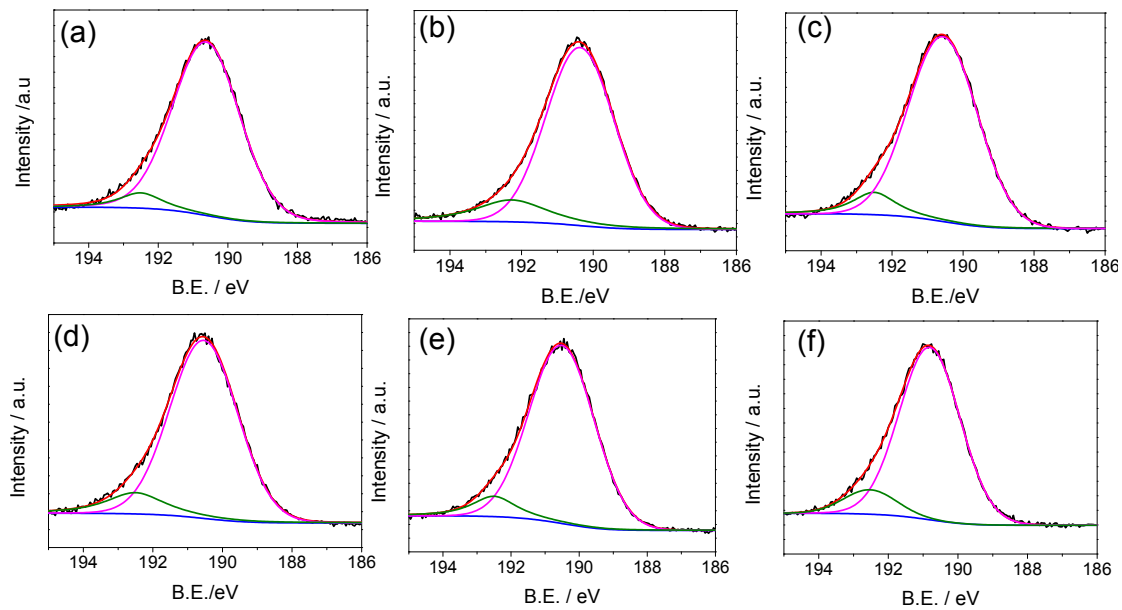


Fig. S6 B1s core-level spectra

Sample order: a) BN-M₃₀; b) BN-M₁₅; c) BN-E₃₀; d) BN-P₃₀; e) BN-W₃₀; f) BN-B₃₀.

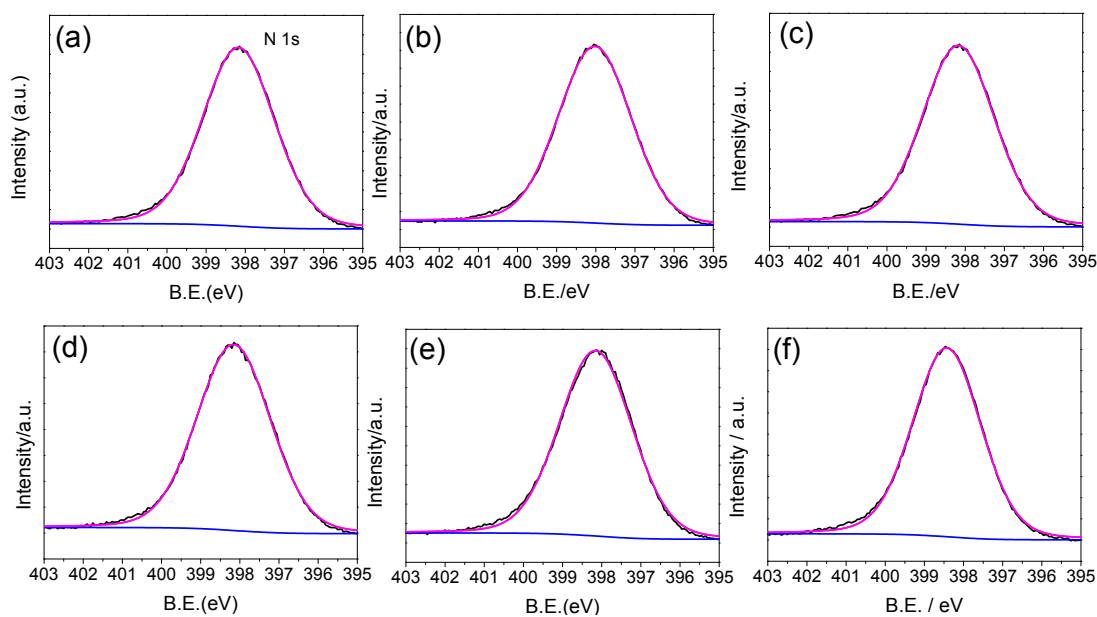


Fig. S7 N1s core-level spectra

Sample order: a) BN-M₃₀; b) BN-M₁₅; c) BN-E₃₀; d) BN-P₃₀; e) BN-W₃₀; f) BN-B₃₀.

Table S1 Binding Energies of B and N in all h-BNNs samples

Elements		BN-M ₁₅	BN-M ₃₀	BN-E ₃₀	BN-P ₃₀	BN-W ₃₀	BN-B ₃₀
B (eV)	B-N	190.4	190.5	190.4	190.5	190.8	190.4
	B-O	192.5	192.5	192.5	192.4	192.4	192.5
N (eV)	N-B	398.1	398.2	398.1	398.1	398.0	398.0

Binding energies (B.E.) of B and N for all samples are around 190.4-190.5 eV and 398.0-398.2 eV, respectively, close to previous reports for hexagonal layers with BN₃ and NB₃ trigonal units.^{S[1]} The peaks around 192.5 eV are attributed to B-O bonds from precursors, which may be presence of -OH on h-BNNs.^{S[2]} Molar ratios of B and N are about 1.06:1, consistent with theoretical values.

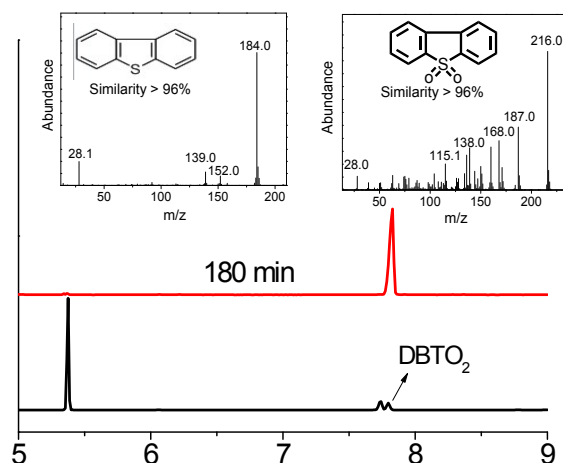


Fig. S8 Gas Chromatography-Mass Spectrometer(GC-MS) of reextracted BN-M₃₀ phase using diethyl ether.

Reaction conditions: $m(\text{catal.}) = 100 \text{ mg}$; $V(\text{model oil}) = 40 \text{ mL}$; $T = 150^\circ\text{C}$; $V(\text{air}) = 100 \text{ mL}\cdot\text{min}^{-1}$.

To prove the proposed reaction mechanism, gas chromatography-mass spectrometer (GC-MS) was used to analyze oxidized product in h-BNNs and the results are presented in Fig. S8. When the aerobic catalysis oxidation of DBT reaction was carried out to 60 min and 180 min (after reaction), the BN-M₃₀ was carefully separated and centrifuged respectively. Then the h-BNNs phase was reextracted by diethyl ether and injected into GC-MS to analyze the composition. As we can see from Fig. S8 that when reaction carried out to 60 min, large amount of DBT can be detected while few amount of oxidized product, DBTO and DBTO₂, can be seen. When the reaction was finished, almost no DBT and DBTO exist in h-BNNs while increasing amount of DBTO₂ appeared, indicating that nearly all DBT was aerobic oxidized to DBTO₂. DBTO is a active intermediate, whose formation is not the reaction determine step (*RSD*).

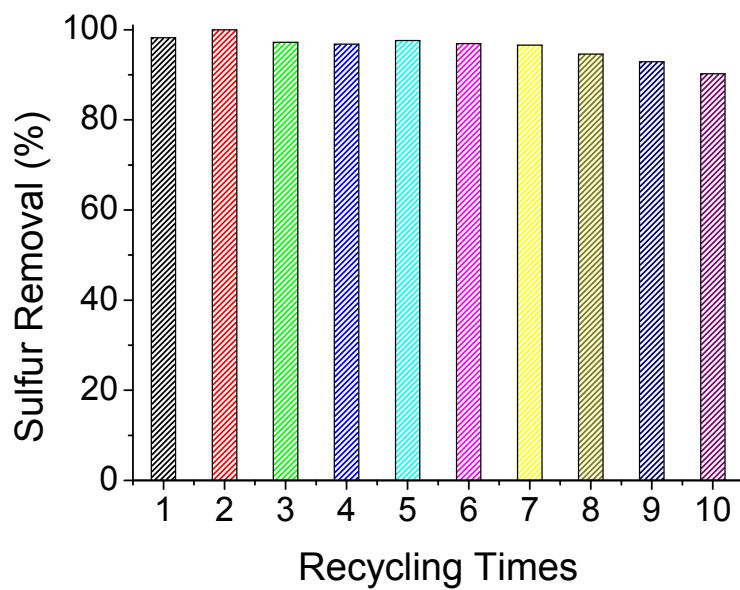


Fig. S9 Recycling performance of M-BN₃₀ in aerobic catalytic oxidation of DBT

Reaction conditions: $m(\text{catal.}) = 100 \text{ mg}$; $V(\text{model oil}) = 40 \text{ mL}$; $T = 150^\circ\text{C}$; $V(\text{air}) = 100 \text{ mL}\cdot\text{min}^{-1}$.

Reference:

S1 W. W. Lei, H. Zhang, Y. Wu, B. Zhang, D. Liu, S. Qin, Z. Liu, L. Liu, Y. Ma, Y. Chen, *Nano Energy* 2014, **6**, 219-224.

S2 W. W. Lei, D. Portehault, R. Dimova, M. Antonietti, *J. Am. Chem. Soc.* 2011, **133**, 7121-7127.